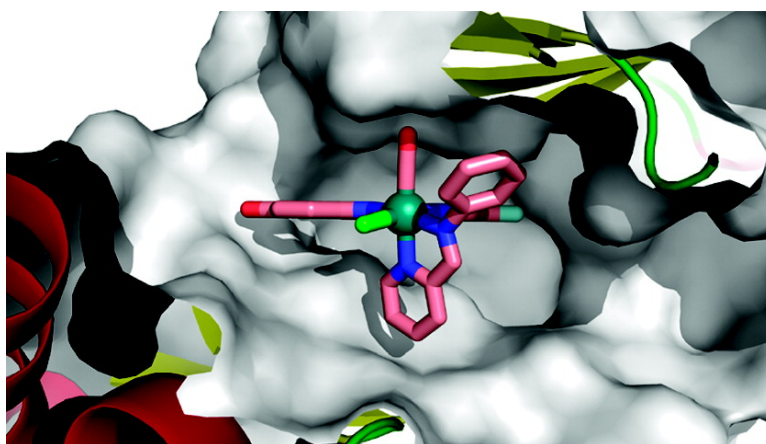


Targeting Large Kinase Active Site with Rigid, Bulky Octahedral Ruthenium Complexes

Jasna Maksimoska, Li Feng, Klaus Harms, Chunling Yi,
Joseph Kissil, Ronen Marmorstein, and Eric Meggers

J. Am. Chem. Soc., **2008**, 130 (47), 15764-15765 • DOI: 10.1021/ja805555a • Publication Date (Web): 31 October 2008

Downloaded from <http://pubs.acs.org> on February 8, 2009



More About This Article

Additional resources and features associated with this article are available within the HTML version:

- Supporting Information
- Access to high resolution figures
- Links to articles and content related to this article
- Copyright permission to reproduce figures and/or text from this article

[View the Full Text HTML](#)



ACS Publications
High quality. High impact.

Targeting Large Kinase Active Site with Rigid, Bulky Octahedral Ruthenium Complexes

Jasna Maksimoska,^{†,‡} Li Feng,[§] Klaus Harms,[§] Chunling Yi,[†] Joseph Kissil,[†] Ronen Marmorstein,^{*,†,‡} and Eric Meggers^{*,§}

Philipps-Universität Marburg, Fachbereich Chemie, Hans-Meerwein Strasse, D-35043 Marburg, Germany, and University of Pennsylvania, Department of Chemistry and The Wistar Institute, Philadelphia, Pennsylvania 19104

Received July 24, 2008; E-mail: meggers@chemie.uni-marburg.de; marmor@wistar.org

The development of selective enzyme inhibitors is at the heart of chemical biology and medicinal chemistry. This is a particularly formidable challenge for members of large enzyme families with homologous active sites such as protein kinases that contain over 500 protein members with highly conserved ATP binding sites.^{1,2} Here, we present a new strategy for the design of selective protein kinase inhibitors that makes use of a discrimination between the size of the ATP binding site through the use of rigid, bulky ruthenium complexes.

Our laboratory recently demonstrated that inert metal complexes can serve as promising scaffolds for the design of enzyme inhibitors.³ Based on these studies, we hypothesized that octahedral complexes in particular should be uniquely suited to selectively target large active sites by establishing rigid shapes that can be easily varied in size by assembling a structure from a single center and changing the nature of the coordinating ligands. As a model system to test this approach we chose the p21-activated kinase 1 (PAK1) which is known to contain an especially open ATP binding site.⁴

An initial screening of a small library of 48 ruthenium complexes led to the identification of the GSK3 and Pim1 half-sandwich inhibitors **NP309** and **DW12** as the most potent compounds for PAK1 with IC₅₀ values of ~1 μM (Figure 1, Table 1). A subsequent cocrystal structure of (*R*)-**DW12** with the kinase domain of PAK1 (amino acids 249–545, inactivating mutation Lys299Arg) at 2.35 Å resolution revealed the important determinants for this affinity: the maleimide moiety and the indole OH-group together mediate four hydrogen bonds to the backbone of the hinge region (Figure 2). In addition, the monodentate carbonyl ligand establishes interactions to residues of the glycine-rich loop. Most interestingly, the η⁵-cyclopentadienyl moiety is not in close contact with any amino acid side chain of the protein, thus highlighting the large amount of vacant space accessible in the PAK1 active site that is not available in many other kinases such as Pim1 and GSK3.

To elaborate compounds to fill the vacant space of the PAK1 ATP binding site, we prepared octahedral complexes **1** that contain the pyridocarbazole moiety and CO ligand of **NP309** (Figure 3). Accordingly, pyridocarbazole **2** was cyclometallated with [(η⁶-benzene)RuCl₂]₂ in the presence of K₂CO₃ providing the η⁶-half-sandwich complex **3** (88%). The benzene was next replaced by three acetonitrile molecules upon UV-photolysis in acetonitrile, followed by TBS-deprotection with TBAF, affording complex **4** diastereoselectively in 41% yield over two steps, which was subsequently used as a general precursor for the synthesis of a variety of octahedral complexes **1**.⁵

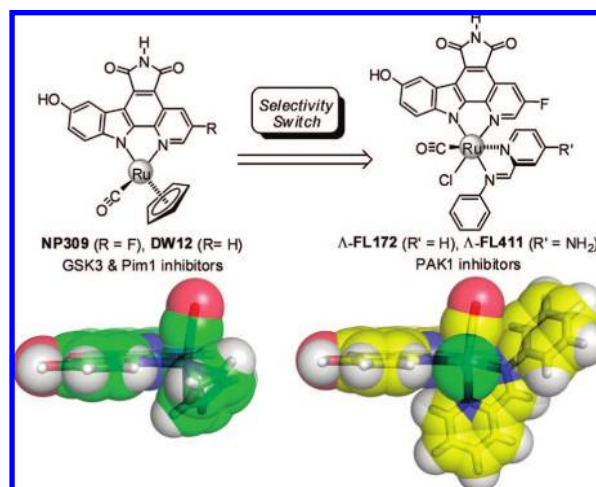


Figure 1. Kinase selectivity switch by the transformation of a small half-sandwich scaffold into rigid, bulky octahedral ruthenium complexes.

Table 1. IC₅₀ values in nM of **DW12**, **NP309**, **FL172**, and **FL411** against GSK3β, Pim1, and PAK1^a

	GSK3β	Pim1	PAK1
<i>rac</i> - DW12	0.32 ± 0.03	0.14 ± 0.01	1090 ± 80
<i>rac</i> - NP309	0.28 ± 0.04	0.17 ± 0.02	770 ± 70
Δ- FL172	440 ± 30	140 ± 23	3480 ± 220
Δ- FL172	1480 ± 60	440 ± 15	130 ± 10
Δ- FL411	1930 ± 90	470 ± 15	5200 ± 815
Δ- FL411	14400 ± 1600	2840 ± 200	110 ± 10

^a IC₅₀ values obtained by phosphorylation of substrates with [γ-³²P]ATP in the presence of 1 μM ATP (IC₅₀ ≈ K_i). All experiments were run in triplicate. K_m values for ATP (in μM): GSK3β = 9.3 ± 0.8, Pim1 = 48 ± 6, PAK1 = 4.4 ± 0.3.

We found that the reaction of **1** with CO (DMF, 75 °C, 1 h) and then with 2-(*N*-phenylaminomethyl)pyridine (DMF, 95 °C, 2 h) without prior workup yielded, under complete diastereoselectivity and oxidation of the amine, the racemic complex **FL172** (Figure 1). Out of a library of ~20 compounds, **FL172** was the most promising inhibitor for PAK1. Testing of racemic **FL172** against a panel of 264 protein kinases revealed that at a concentration of 3 μM (10 μM ATP) only 15 kinases (5.7% of total) displayed an activity of less than 20%, including PAK1, GSK3, and Pim1 (see Supporting Information). **FL172** was resolved into the Δ- and Δ-enantiomers by chiral HPLC, and the individual isomers were tested against Pim1, GSK3, and PAK1.⁶ The IC₅₀ values in Table 1 reveal a strong modulation in selectivity with the Δ-enantiomer of **FL172** being 27-fold more potent for PAK1 compared to Δ-**FL172**. Through a subsequent structure–activity study we obtained Δ-**FL411**, bearing an additional amino group (Figure 1),

[†] The Wistar Institute.

[‡] University of Pennsylvania.

[§] Philipps-Universität Marburg.

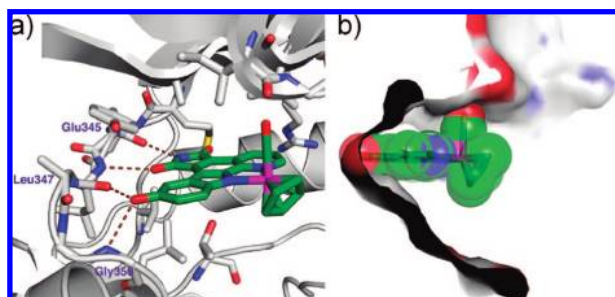


Figure 2. Cocystal structure at 2.35 Å of (*R*)-**DW12** with PAK1 (249–545, mutation Lys299Arg). (a) H-bonding interactions between (*R*)-**DW12** and PAK1. (b) Surface view through the active site illustrating the open ATP-binding site of PAK1.

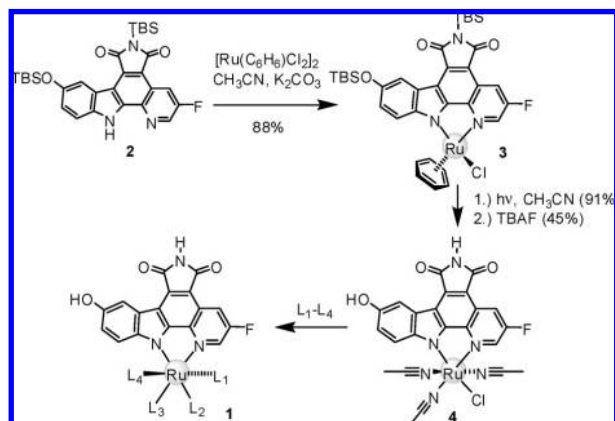


Figure 3. Synthesis of octahedral Ru complexes **1** from precursor **4**.

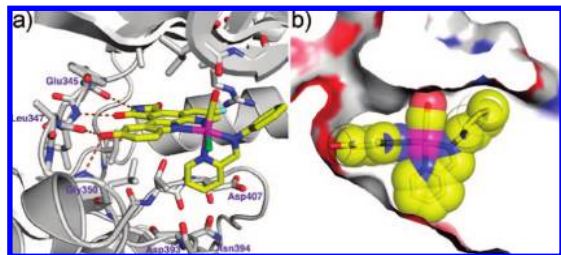


Figure 4. Cocystal structure of Δ -**FL172** with PAK1 (amino acids 249–545, mutation Lys299Arg) at 1.65 Å. (a) H-bond interactions. (b) Surface view illustrating the shape complementarity of PAK1 and Δ -**FL172**.

which further significantly improves relative affinity for PAK1 (110 nM) over Pim1 (2.84 μ M) and GSK3 (14.4 μ M) (Table 1). Thus by just replacing the cyclopentadienyl moiety in **NP309** for a chloride and a bulky, rigid bidentate phenyliminopyridine ligand in Δ -**FL411**, the initial picomolar affinities for Pim1 and GSK3 dropped by factors of 16 700 and 51 400, respectively, whereas at the same time the affinity for PAK1 improves by almost 1 order of magnitude.

The 1.65 Å resolution cocystal structure of Δ -**FL172** bound to PAK1 reveals the molecular details of the binding of this octahedral scaffold to PAK1. Whereas the pyridocarbazole moiety and CO ligand bind analogously to (*R*)-**DW12**, the bulky bidentate iminopyridine ligand now stretches the entire distance from the N-terminal glycine-rich loop to the C-terminal domain (Figure 4). In this bulky octahedral complex the distance between the oxygen atom of the CO ligand and the *para*-carbon of the pyridine in *trans* serves as a rigid yardstick of \sim 8 Å which is well accommodated by the active site of PAK1, but not most other protein kinases.

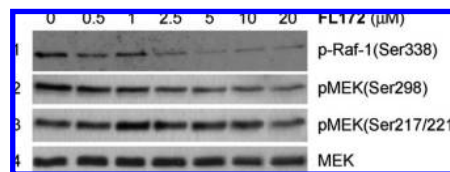


Figure 5. Kinase inhibition with racemic **FL172** in RT4 rat schwannoma cells. Serum-starved RT4 cells were treated with **FL172** at indicated concentrations for 1 h and then stimulated with 10 ng/mL PDGF for 5 min. PAK1 inhibition was monitored by levels of Ser338-phosphorylated Raf-1 and Ser298-phosphorylated MEK analyzed by Western blot with an antiphospho-Raf-1(Ser338) (entry 1) and antiphospho-MEK(Ser298) antibody (entry 2), respectively. Antibodies against phospho-MEK(Ser217/221) (entry 3) and endogenous levels of total MEK served as controls (entry 4). Lane 1 was generated in an independent experiment.

Finally, to assess the biological activity of **FL172**, we investigated its ability to interfere with PAK1 activity within mammalian cells. The Western blot in Figure 5 demonstrates that the phosphorylation of the endogenous PAK1 substrate MEK at Ser298 was reduced with increasing concentration of racemic **FL172**, whereas the other MEK phosphorylation sites Ser217 and Ser221, which are not directly phosphorylated by PAK1, were not considerably affected.⁷ Similarly, phosphorylation of Ser338 on endogenous Raf-1⁸ could be suppressed in a concentration dependent manner, consistent with intracellular PAK1 inhibition by **FL172**, but not ruling out additional intracellular targets (Figure 5).

PAK1 is implicated in tumorigenesis and metastasis, and pharmacological inhibitors of PAK1 are thus promising candidates for cancer therapy.⁹ However, to the best of our knowledge, there are no selective organic inhibitors with IC₅₀ values in the nanomolar range known for PAK1 or other group-I PAK kinases.^{9,10} The bulky organoruthenium compound Δ -**FL411** constitutes a promising lead structure for the generation of improved PAK1 inhibitors by functionalizing the associated ligands in a combinatorial and structure-based fashion. Work along these lines is in progress.

Acknowledgment. Financial support from the National Institutes of Health (GM071695) and the Philipps-University Marburg are gratefully acknowledged.

Supporting Information Available: Experimental details, analytical data, crystallographic data, kinase inhibition profiles, cellular assays. This material is available free of charge via the Internet at <http://pubs.acs.org>.

References

- (1) Manning, G.; Whyte, D. B.; Martinez, R.; Hunter, T.; Sudarsanam, S. *Science* **2002**, *298*, 1912–1934.
- (2) For recent successful approaches, see for example: (a) Bishop, A. C.; Kung, C.-y.; Shah, K.; Witucki, L.; Shokat, K. M.; Liu, Y. *J. Am. Chem. Soc.* **1999**, *121*, 627–631. (b) Cohen, M. S.; Zhang, C.; Shokat, K. M.; Taunton, J. *Science* **2005**, *308*, 1318–1321.
- (3) For an account, see: Meggers, E.; Atilla-Gokcumen, G. E.; Bregman, H.; Maksimoska, J.; Mulcahy, S. P.; Pagano, N.; Williams, D. S. *Synlett* **2007**, *8*, 1177–1189.
- (4) Lei, M.; Lu, W.; Meng, W.; Parrini, M.-C.; Eck, M. J.; Mayer, B. J.; Harrison, S. C. *Cell* **2000**, *102*, 387–397.
- (5) For a related precursor, see: Bregman, H.; Carroll, P. J.; Meggers, E. *J. Am. Chem. Soc.* **2006**, *128*, 877–884.
- (6) The relative configuration of **FL172** was established by X-ray crystallography of a derivative and the absolute configurations of the Δ - and Λ -enantiomers from the cocystal structure with PAK1.
- (7) Frost, J. A.; Steen, H.; Shapiro, P.; Lewis, T.; Ahn, N.; Shaw, P. E.; Cobb, M. H. *EMBO J.* **1997**, *16*, 6426–6438.
- (8) Tran, N. H.; Frost, J. A. *J. Biol. Chem.* **2003**, *278*, 11221–11226.
- (9) Kumar, R.; Gururaj, A. E.; Barnes, C. J. *Nat. Rev. Cancer* **2006**, *6*, 459–471.
- (10) For an allosteric PAK1 inhibitor, see: Deacon, S. W.; Beeser, A.; Fukui, J. A.; Rennefahrt, U. E. E.; Myers, C.; Chernoff, J.; Peterson, J. R. *Chem. Biol.* **2008**, *15*, 322–331.

JA805555A